

Simplified method for prediction of elastic-plastic buckling strength of web-post panels in castellated steel beams

Mei Liu^{1a}, Kangrui Guo^{1,2}, Peijun Wang^{*1}, Chao Lou¹ and Yue Zhang³

¹School of Civil Engineering, Shandong University, Jinan, Shandong Province, 250061, China

²Shandong Urban and Rural Planning Design Institute, Jinan, Shandong Province, 250061, China

³Shanghai Construction No. 1 (Group) Co. LTD, Shanghai, 200120, China

(Received April 22, 2017, Revised July 19, 2017, Accepted September 2, 2017)

Abstract. Elastic-plastic shear buckling behaviors of the web-post in a Castellated Steel Beam (CSB) with hexagonal web openings under vertical shear force were investigated further using Finite Element Model (FEM) based on a sub-model, which took the upper part of the web-post under horizontal shear force to represent the whole web-post under vertical shear force. A simplified design method for the web-post elastic-plastic shear buckling strength was proposed based on simulation results of the sub-model. Proper boundary conditions were applied to the sub-model to assure that its behaviors were identical to those of the whole web-post. The equation to calculate the thin plate elastic shear buckling strength was adopted as the basic form to build the design equation for elastic-plastic buckling strength of the sub-model. Parameters that might affect the elastic-plastic shear buckling strength of the whole web-post were studied. After obtaining the vertical shear buckling strength of a sub-model through FEM, the shear buckling coefficient k can be obtained through the back analysis. A practical calculation method for k was proposed through curving fitting the parameter study results. The elastic-plastic shear buckling strength of the web-post calculated using the proposed shear buckling coefficient k agreed well with that obtained from the FEM and test results. And it was more precise than those obtained from EC3 based on the strut model.

Keywords: castellated steel beam; web-post; elastic-plastic shear buckling; plate shear buckling coefficient; design method

1. Introduction

The castellated steel beam (CSB) can be made through cutting an H-section steel beam in a zig-zag pattern along the web and then re-welding the two parts together at the convex area. The floor thickness of the building can be reduced by installing the service pipelines in web openings. The buckling of beam web-post would be commonly encountered especially for the CSBs with great web height to thickness ratio. Lawson and Hicks (2005) described developments in composite construction and their effect on codified design procedures in the UK. Areas of particular interests included: rules on shear connection, the design of beams with web openings, serviceability limits, such as floor vibrations, and the fire safe design. Ellobody (2011) investigated behaviors of a CSB under the combined lateral torsional and distortional buckling modes. Finite element simulation results showed that the presence of web distortional buckling caused a considerable reduction in the load carrying capacity of the slender CSB. Abidin *et al.* (2017) presented an approach which provided the necessary input for local out-of-plane buckling analysis of web components. Abidin and Izzuddin (2013) considered the

efficient local buckling analysis of beams with regular and irregular web openings, employing the Element Free Galerkin method for the numerical discretization together with a simplified buckling assessment approach from the Rotational Spring Analogy. The new approach provided significant computational benefits for beams with regular repeated cells. Erdal and Saka (2013) carried out experimental studies on twelve full-scale non-composite cellular beams. In addition to web buckling, the Vierendeel bending occurred on the tested beams. Test results showed that if the buckling strength of the web was not sufficient to carry imposed concentrated load filling the openings and using of longitudinal, transverse or ring stiffeners should be considered to increase loaded area at the center of the beam. Kaveh and Shokohi (2015) proposed an optimum design of laterally-supported castellated beams using colliding body optimization algorithm. It could be concluded that the use of beam with hexagonal opening required smaller amount of steel material and it was superior to the cellular beam from the cost point of view. Yang *et al.* (2016) carried out experimental studies on shear performance of partially precast castellated steel reinforced concrete beams. Based on the test results, the shear failure mechanism was revealed, and the effect of the concrete strength and shear span-to-depth ratios were investigated. The shear capacity of such kind of precast castellated steel reinforced concrete beam was furthermore discussed, and the influences of the holes on the steel shape on the shear performance were particularly analyzed. Durif *et al.* (2015) carried out

*Corresponding author, Ph.D.

E-mail: pjwang@sdu.edu.cn

^aPh.D.

E-mail: Liumei@sdu.edu.cn

experimental tests on cellular beams with sinusoidal openings. Test results showed the formation of four plastic hinges and the local instability of the sinusoidal part of the opening. An approach to quantify this rotational restraint was proposed. Kaveh and Shokohi (2016a, 2016b) and Kaveh and Ghafari (2016a, 2016b) proposed a series of optimization algorithm for the design of castellated beams, such as the meta-heuristic algorithm for beams with/without end-filled holes (Kaveh and Shokohi 2016a), the colliding bodies optimization and particle swarm optimization for beams with hexagonal openings and beams with circular openings (Kaveh and Shokohi 2016b), and floor optimization for decreasing the total cost of the floor (Kaveh and Ghafari 2016, 2017). For the web openings break the continuity of the beam web, castellated beams might be failed by web-post buckling or Vierendeel Mechanism failure at the perforated section. Kerdel *et al.* (1984) investigated all the potential failure modes of a castellated steel beam, including Vierendeel mechanism, web post buckling and web weld rupture. Research results showed that currently available methods were adequate for design except for the case of web post buckling.

An inclined compression strut would be formed in the web-post under vertical shear force, as shown in Fig. 1(a). BS5950 (2000) proposed a strut model to calculate the buckling strength of the web-post, in which the stability of the compression strut was checked by the column buckling curve “c”. Lawson *et al.* (2006) presented a simplified equation for calculating the web-post shear buckling strength based on the strut model, which was calibrated against results of finite element analyses. The simplified equation was applicable to a CSB with cellular openings, while it was not accurate enough in calculating the CSB with other opening shapes. Wang *et al.* (2014a) proposed a modification to the strut model for predicting the shear buckling capacity of the web-post in the CSB with fillet corner openings. Tsavdaridis and D’Mello (2011) carried out experimental and analytical studies on two beams with circular web openings and five perforated beams with novel web opening shapes to investigate the failure mode and shear buckling strength of the web-post. An empirical formula to predict the ultimate vertical shear buckling strength of web-posts was formulated for the particular web opening shapes. Panedpojaman *et al.* (2014) proposed novel design equations for shear strength of local web-post buckling in cellular beams. The design was based on the strut model and codes of EC3 (2005) and the strut length incorporated restraint effects of the tee depth and the stress variation.

Although the strut model had been widely used to calculate the shear buckling strength of a web-post, it had theoretical discordance. In the first, under vertical shear force, the web-post torsional buckled in an “S” shape instead of flexural buckling in a double curvature, which was discordant to assumptions of the column curve “c”. Secondly, the beneficial effect of the inclined tension zone to the buckling resistance of the compression strip was not included in the model. And thirdly, the effective width and length of the strut was calculated by empirical formula which was not accurate enough.

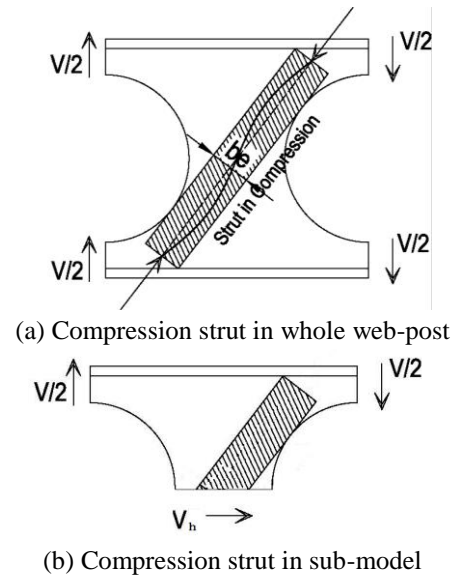


Fig. 1 Compression strut in web-post

Other than predicting the shear buckling strength of the web-post through the inclined strut, the shear buckling strength of a web-post could also be obtained through a sub-model under horizontal shear force, as shown in Fig. 1(b).

The buckling strength of the sub-model could be obtained through the thin plate shear buckling theory. The upper part of the web-post under horizontal shear force was adopted as sub-model to represent the whole web-post under vertical shear force, as shown in Fig. 1(b). The buckling strength of the sub-model could be obtained through the thin plate shear buckling theory. Since the critical loads were not sensitive to flange dimensions, the sub model did not include the flange.

Redwood and Demirdjian (1998) investigated elastic buckling behaviors of the web-post in the CSB with hexagonal openings through studying the upper part of the web-post under horizontal shear force. The horizontal shear buckling strength, $V_{h,cr}$, of the sub-model was calculated by

$$V_{h,cr} = k \frac{Eet_w}{(h_0/t_w)^2} \quad (1)$$

where k was the shear buckling coefficient of the upper part of the web-post under horizontal shear force. E was the Young’s modulus of steel. e was the width of web-post. t_w was the web-post thickness. h_0 was the height of web opening. From the force equilibrium of the sub-model, the vertical shear buckling strength of the web-post was calculated by

$$V_{cr} = \frac{h - 2y_i}{s} V_{h,cr} \quad (2)$$

where h was the section height of CSB. y_i was the distance from the flange to the centroid of Tee-section. s was the distance between two adjacent web openings. For a certain CSB, k was the only unknown parameter in Eq. (1). The shear buckling coefficient k proposed by Redwood and Demirdjian (1998) could be only used to calculate the elastic shear buckling strength of a CSB with hexagonal

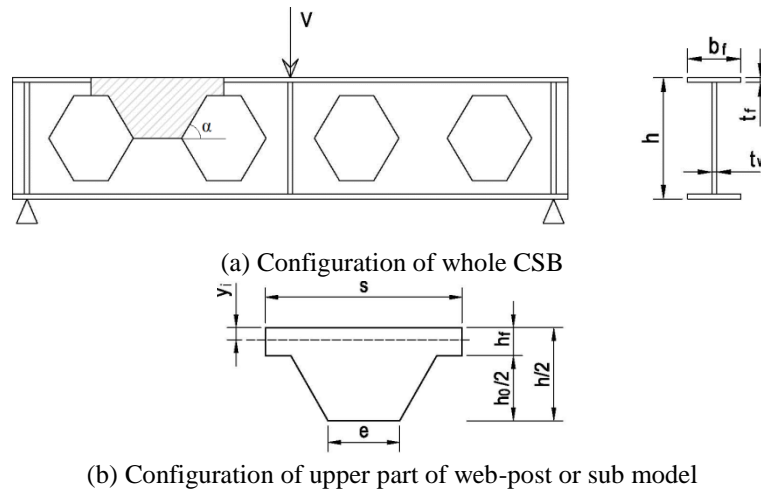


Fig. 2 Configuration of studied CSB

web openings. For a CSB with other web opening shapes and being failed by elastic-plastic shear buckling, a new shear buckling coefficient k should be proposed.

Substituting Eq. (1) into Eq. (2), the vertical shear buckling strength of the web-post can be obtained by

$$V_{cr} = k \cdot \frac{h - 2y_i}{s} \cdot \frac{Eet_w}{(h_0/t_w)^2} \quad (3)$$

As an extension of previous studies (Wang *et al.* 2016) on elastic shear buckling behaviors of the web-post in a CSB with hexagonal web openings under vertical shear force, the elastic-plastic shear buckling behaviors of the web-post were further investigated using Finite Element Model (FEM) based on a sub-model. The shear buckling coefficient k , for the elastic shear buckling design, was affected by the opening height to web thickness ratio h_0/t_w , the web-post width to web thickness ratio e/t_w , the web height of Tee-section above the opening to the web thickness h_f/t_w , the web thickness t_w and the inclination angle of the opening edge α . Whether the design method for k proposed by Wang *et al.* (2016) was applicable for the elastic-plastic shear buckling analysis of the web-post was not clear and needed investigated further. If necessary a new design equations for k should be proposed.

The CSB may also fail in Vierendeel mechanism at the perforated section before the web-post shear buckling when a CSB had a great h_0/t_w . Based on analytical and numerical studies, Chung *et al.* (2011), Liu and Chung (2003) proposed empirical $M-V$ interaction curves at the perforated sections for the Vierendeel mechanism failure. Wang *et al.* (2014b) investigated effects of opening dimensions and opening shapes on the Vierendeel failure of CSBs with fillet corner web openings and proposed a practical design method. Panedpojaman *et al.* (2015) proposed an interaction curve to check the Vierendeel failure of non-composite symmetric cellular beams, or steel beams with circular or elongated circular openings, which was based on a quadratic nonlinear failure criterion.

In this paper, a simplified calculation method for the elastic-plastic shear buckling strength of the web-post based on the sub-model was proposed. After obtaining the elastic-

plastic shear buckling strength of the web-post through FEM simulation, the shear buckling coefficient k was calculated through back analysis. And then an equation was proposed to calculate k based on the parameter study results. Studies in this paper followed four steps:

(1) a FEM for the whole web-post model and the sub-model was proposed and verified by available test results (Wang *et al.* 2014a) on CSBs failed in web-post buckling;

(2) the shear buckling strength obtained from the whole web-post model and the sub-model were compared to prove the applicability of the sub-model in calculating the buckling strength of a web-post in elastic-plastic stage;

(3) parameters affected the shear buckling coefficient k of the web-post in elastic-plastic stage were studied; and then an equation to calculate k was proposed;

(4) the vertical elastic-plastic shear buckling strength of the web-post obtained using the proposed buckling coefficient k was verified by FEM and test results (Redwood and Demirdjian 1998, Zaarour and Redwood 1996). The calculated results were also compared with those calculated by EC3 (2005) to show the precision of the proposed method.

2. Finite element model and verification

2.1 Model description

The CSBs studied were made of Q345 steel with yield strength of 345 MPa and Poisson's ratio of 0.3. The material behavior was described using the PLASTIC option in ABAQUS (2008) that allowed a nonlinear stress-strain curve to be used. Elastic-perfectly plastic model was used to define the material properties in this paper. No strain hardening was included. The first part of the nonlinear curve represented the elastic part up to the proportional limit stress with Young's modulus of 210 GPa, as described in EC3 (2005). Since the non-linear buckling analysis involved large inelastic strains, the nominal stress-strain curves were converted to true stress and logarithmic plastic true strain curves. The steel constitutive model in the proposed FEM used Von Mises yield surfaces with

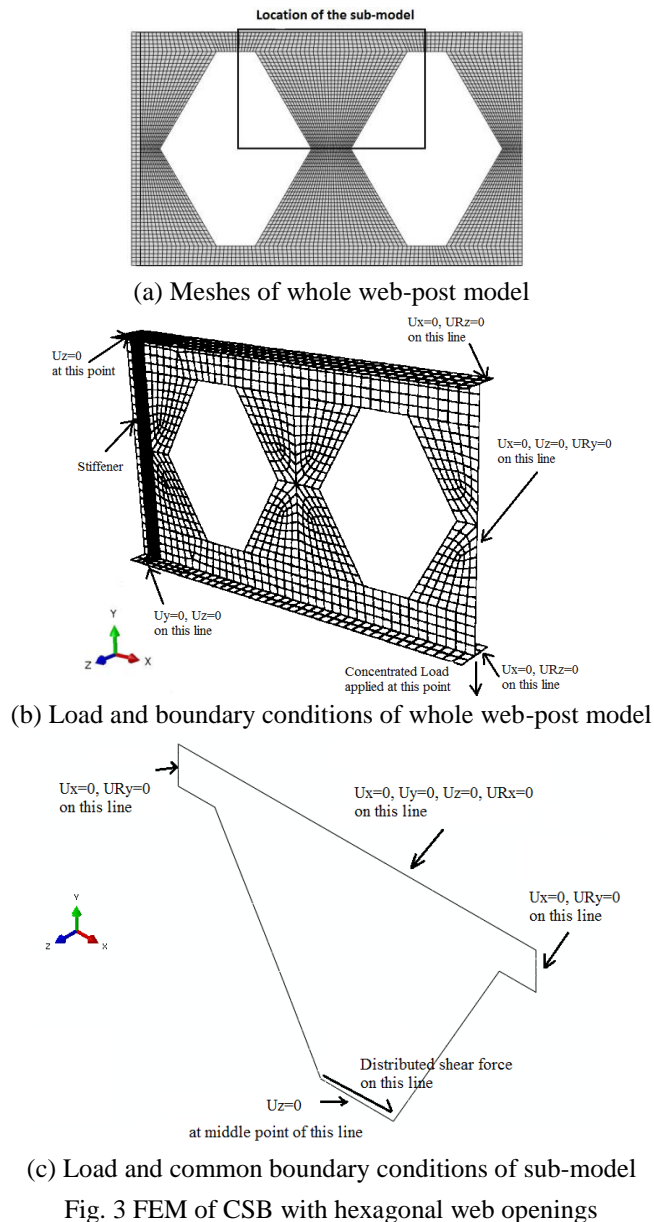


Fig. 3 FEM of CSB with hexagonal web openings

associated plastic flow, which allowed for isotropic yield and was defined by giving the value of uniaxial yield stress as a function of uniaxial equivalent plastic strain (Zaarour and Redwood 1996, EC3 2005).

The whole web-post model had two openings along the beam, as shown in Fig. 2. The vertical concentrated force was applied at the middle span of the beam. The width and thickness of the two flanges were 180 mm and 20 mm, respectively.

Only the web in the sub-model was modeled. Effects of the top flanges to the web-post were represented by rotational and transitional restraints. α was the inclination angle of web opening edge. h_f was the web height of the Tee-section above the web opening. l was the half span of the CSB. t_f was the thickness of the flange. h and b_f were the section height and flange width of the CSB.

Initial geometrical imperfection was inevitable in a CSB as a result of cutting and welding process. The first buckling mode of BUCKLE analysis in ABAQUS was used

Table 1 Boundary conditions of sub-model with different dimensions

Specimens	t_w (mm)	e (mm)	h_0 (mm)	h_f (mm)	α	BCs of bottom edge	V_{sub} (kN)	V_{whole} (kN)	$V_{sub}/$ V_{whole}
Group 1	5	200	500	100	60°	UR _x =0	160.1	160.6	0.99
Group 2	8	320	640	200	60°	UR _x = UR _z =0	380.5	376.8	1.01
Group 3	12	240	960	144	60°	UR _y =0	535.5	538.6	0.99

as the initial imperfection with the 1mm of maximum out-of-plane displacement magnitude (Wang *et al.* 2014a).

2.2 Boundary conditions

For the symmetry of the whole web-post model, only half of the beam was modeled, as shown in Fig. 3(a). Displacements in y (U_y) and z (U_z) direction of the bottom flange at the left end of the beam were restrained to simulate the pin support. The U_z at the top flange was restrained to simulate the lateral brace. At the right end of the beam, the displacement in x (U_x) direction and the rotation around y -axis (UR_y) of the web were restrained. The U_z was also restrained to prevent the beam from failing at the lateral torsional buckling. For the top and bottom flanges, the U_x and the rotation around z -axis (UR_z) were restrained. The vertical shear force was applied at the bottom flange, as shown in Fig. 3(b).

In the sub-model, the U_x , U_y , U_z and the rotation around x -axis (UR_x) of the top edge were restrained to simulate the restraint provided by the flange. The U_x and UR_y of the left and right edge were restrained to simulate the restraint provided by the adjacent web. For the sub-models, the U_z at the middle point of the bottom edge was fixed, as shown in Fig. 3(c). The restraints to the bottom edge provided by the adjacent web might change with the changing of the web-post dimensions. Three specimens were used to illustrate the different rotational restraints to the bottom edge of the sub-model, as listed in Table 1. A distributed horizontal shear force was applied on the bottom edge, as shown in Fig. 3(c). The shear load was applied through shell edge load in the sub-model, which was assumed to be uniformly distributed along the line, as shown in Fig. 3(c).

The whole web-post model and the sub-model both were meshed using the shell element S4R in ABAQUS, a 4-node quadrilateral shell element with reduced integration and a large-strain formulation, with mesh size of 10×10 mm. The eigenvalue buckling analysis was employed to obtain the elastic buckling strength and the buckling modes of the web-post.

2.3 Model verification

Tests results on CSBs failed in web-post buckling with hexagonal openings by Redwood and Demirdjian (1998), and with hexagonal and octagonal openings by Zaarour and Redwood (1996) were used to verify the FEM of the whole web-post model and the sub-model.

The tested CSBs (Redwood and Demirdjian 1998, Zaarour and Redwood 1996) were simply supported and

Table 2 Tested CSBs with hexagonal openings (Redwood and Demirdjian 1998, Zaarour and Redwood 1996)

Specimens	h (mm)	b_f (mm)	t_w (mm)	t_f (mm)	e (mm)	h_0 (mm)	b (mm)	n	L (mm)	f_{yw} (MPa)	f_{yf} (MPa)
10-5a	380.5	66.9	3.56	4.59	77.8	266.2	76.2	4	1220	352.9	345.6
10-5b	380.5	66.9	3.56	4.59	77.8	266.2	76.2	4	1220	352.9	345.6
10-6	380.5	66.9	3.56	4.59	77.8	266.2	76.2	6	1828	352.9	345.6
10-7	380.5	66.9	3.56	4.59	77.8	266.2	76.2	8	2438	352.9	345.6
10-1	370.59	69.09	3.58	4.39	58.17	245.87	69.85	12	3048	357.1	342
10-3	376.43	70.61	3.61	4.45	57.91	260.53	127	8	3048	357.1	342
12-1	476.25	78.49	4.69	5.33	73.41	352.81	101.6	8	3048	311.6	307
12-3	449.58	78.23	4.62	5.35	71.37	302.51	149.35	6	3048	311.6	307

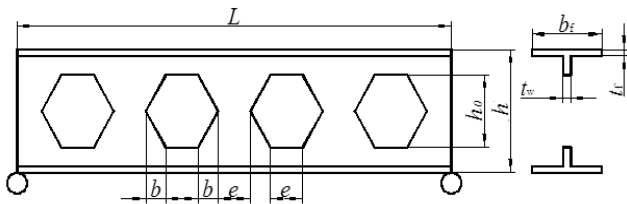


Fig. 4 CSBs with hexagonal openings (Redwood and Demirdjian 1998, Zaarour and Redwood 1996)

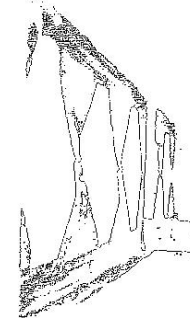
Table 3 Shear buckling strengths of CSBs with hexagonal openings obtained from FEM and test

Specimens	$V_{cr,TEST}$ (kN)	$V_{cr,FEM}$ (kN)	$V_{cr,TEST}/V_{cr,FEM}$	$V_{cr,SUB}$ (kN)	$V_{cr,TEST}/V_{cr,SUB}$
10-5a	46.35	45.75	1.05	43.90	1.05
10-5b	50.45	45.75	1.10	43.90	1.15
10-6	47.4	45.75	1.03	43.90	1.07
10-7	42.2	41.75	1.01	43.90	0.96
10-1	39.55	38.75	1.02	40.67	0.97
10-3	36.92	40.64	0.91	41.40	0.89
12-1	57.33	58.43	0.98	61.7	0.93
12-3	58.22	61.21	0.95	62.3	0.93

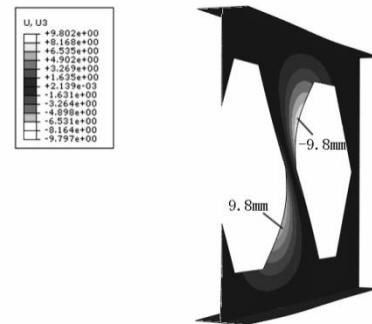
Table 4 Comparison of shear buckling strength obtained by FEM and test

	Beam 10-5(a) (kN)	Beam 10-5(b) (kN)	$(V_{cr,FEM} - V_{cr,Test})/V_{cr,Test}$
Test results (Lawson 2006)	92.7	100.9	
Mean value	96.8		
FEM results (Lawson 2006)	88.6		-8.47%
FEM with 5 mm element type	88.9		-8.16%
S4R and mesh size of 10 mm	91.5		-5.48%
20 mm	91.6		-5.37%

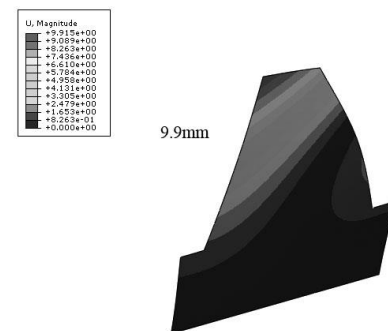
were loaded by a concentrated force at middle span. Vertical stiffeners were applied at the two supports and the loading point at the middle span. Dimensions of tested beams and yield strengths of the web steel (f_{yw}) and the flanges steel (f_{yf}) were listed in Table 2. h was the section height of the CSB. h_0 was the height of web opening. b_f and t_f were the width and thickness of the flange, respectively. t_w was the thickness of the web. e was the width of web-post. b was the horizontal length of the opening edge. L was the length of the beam, as shown in Fig. 4. n was the number of



(a) Test results (Zaarour and Redwood 1996)



(b) FEM results of whole web-post model



(c) FEM results of sub-model model

Fig. 5 Comparison of web-post buckling deformations

openings of the CSB.

Shear buckling strengths obtained from the whole web-post model, the sub-model and tests (Redwood and Demirdjian 1998, Zaarour and Redwood 1996) were listed in Table 3. It could be seen that the shear buckling strengths predicted by the whole web-post FEM and the sub-model FEM agreed well with those measured from tests (Redwood and Demirdjian 1998, Zaarour and Redwood 1996). The $V_{cr,TEST}/V_{cr,FEM}$ varied from 0.91 and 1.05 with a mean value

of 0.99 and a standard deviation of 0.0572. The $V_{cr,TEST}/V_{cr,SUB}$ varied from 0.89 and 1.15.

The model meshed by S4R and three mesh sizes were studied, as shown in Table 4. It can be seen that the shear buckling strength predicted by FEM with mesh size of 10mm agreed very well test results. For beam 10-5a and 10-5b (Redwood and Demirdjian 1998), shear buckling deformations of the web-post obtained from the whole web-post FEM, the sub-model FEM and test were shown in Fig. 5. They agreed well and demonstrated that the web-post buckled in “S” shape

3. Applicability of sub-model on elastic-plastic shear buckling strength of web-post

3.1 Verification of sub-model FEM

Three sub-model FEMs were used in this paper to show their applicability in predicting the web-post elastic-plastic shear buckling strength, as listed in Table 1. The rotational restraints to the bottom edge of sub-model web varied with the changes of web-post dimensions. So unlike that in elastic stage (Wang *et al.* 2016), it would cause wrong predictions on buckling behaviors of a web-post to use fixed boundary conditions to the bottom edge to simulate the rotational restraints provided by the adjacent web.

Buckling strengths obtained from the sub-model FEM were compared with those from the whole web-post FEM. It could be seen that if the proper boundary conditions were used, the buckling behaviors predicted by the sub-model FEM were same with those by the whole CSB FEM. The V_{sub}/V_{whole} varied from 0.99 to 1.01, as listed in Table 1.

3.2 Upper bound of web-post buckling strength

Eq. (3) can be rewritten as

$$k = V_{cr,FEM}/V_{cr,0} \quad (4)$$

$$V_{cr,0} = \frac{h - 2y_i}{s} \cdot \frac{Eet_w}{(h_0/t_w)^2} \quad (4a)$$

After obtaining k , the shear buckling strength of a web-post could be calculated by

$$V_{cr,cal} = kV_{cr,0} \quad (4b)$$

where $V_{cr,FEM}$ was the vertical elastic-plastic shear buckling strength of the web-post, which could be obtained through FEM non-linear buckling analysis. $V_{cr,0}$ was the parameter represented a nominal shear strength depending on the web-post shape. And $V_{cr,cal}$ was the web-post shear buckling strength obtained through the simplified method.

The horizontal elastic-plastic shear buckling strength of the web-post could not exceed its shear yield strength

$$V_{h,p} = 0.58et_w f_y \quad (5)$$

Substitute Eq. (2) and (5) into Eq. (4). The corresponding shear yielding coefficient k_p was

$$k_p = 0.58 \frac{f_y}{E} \left(\frac{h_0}{t_w} \right)^2 \quad (6)$$

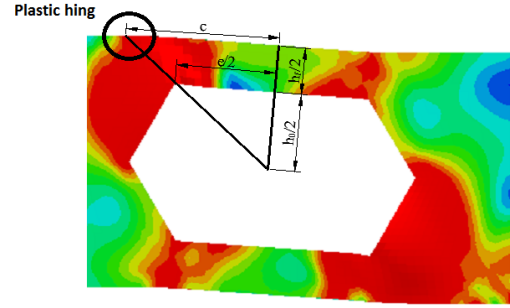


Fig. 6 Effective opening width of CSB with hexagonal openings

On the other hand, a CSB may fail in Vierendeel mechanism at the perforated section. The corresponding load bearing capacity was calculated by

$$\frac{F_v}{2} = \frac{M_{pt}}{c} \quad (7)$$

where c is the effective opening width and M_{pt} is the plastic moment capacity of the top tee-section and calculated as follows

$$M_{pt} = \frac{A_{tee}}{2} \cdot \left(\frac{\bar{x}_1}{2} + \bar{x}_2 \right) \cdot f_y \quad (8)$$

$$A_{tee} = b_f \cdot t_f + h_f \cdot t_w \quad (9)$$

$$\bar{x}_1 = \frac{A_{tee}}{2b_f} \quad (10)$$

$$\bar{x}_2 = \frac{b_f(T - \bar{x}_1)^2 + h_f \cdot t_w [T - \bar{x}_1 + \frac{h_f}{2}]}{\frac{A_{tee}}{2}} \quad (11)$$

$$T = t_f - \bar{x}_1 \quad (12)$$

For a CSB with circular web openings, the effective opening width, c , was calculated by converting the circular web opening into an equivalent rectangular web opening with a width of $0.25d_0$ (Wang *et al.* 2014a). However, this calculated method could not be applied in the CSB with hexagonal openings.

The plastic hinge occurred in the inner corner of hexagonal opening, as shown in Fig. 6. It was more appropriate to calculate the effective opening width, c , by triangle similarity as

$$\frac{c}{e} = \frac{h_0/2 + h_f + t_f}{h_0} \quad (13)$$

The upper bound of web-post shear strength took the minimum value between the capacities corresponding to the Vierendeel failure and the web-post shear yielding failure as

$$V_p = \min \{ V_{h,p}, F_v \} \quad (14)$$

3.3 Assessment of shear buckling coefficient presented in Redwood, 1998

For h_0/h equaling to 0.51 or 0.74, Redwood and

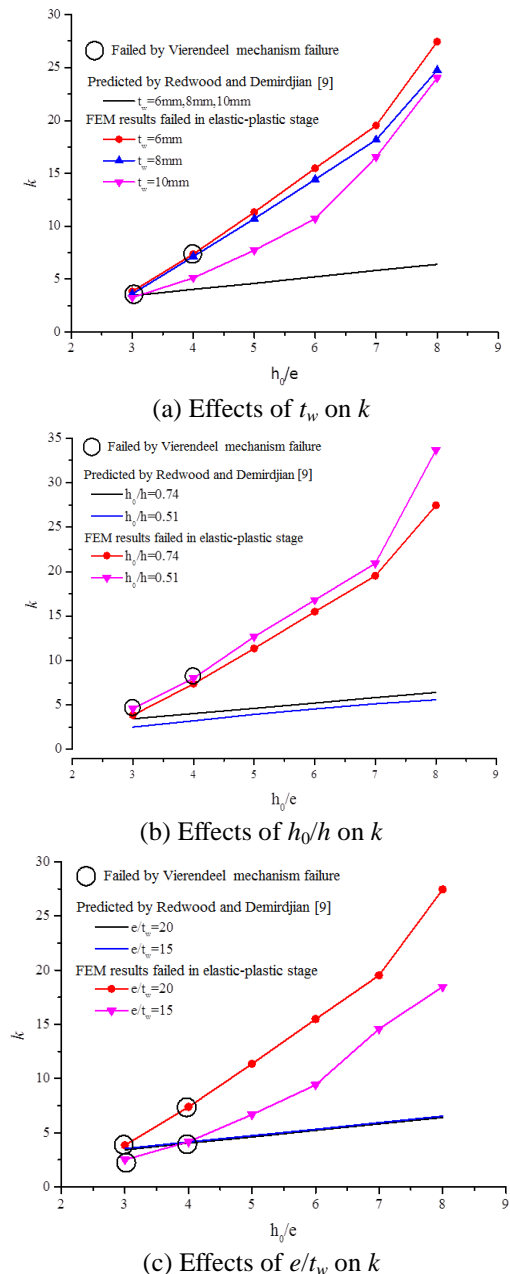


Fig. 7 Values of k obtained from FEM and proposed by Redwood and Demirdjjan (1998)

Demirdjjan (1998) proposed an elastic shear buckling coefficient k as a function of three parameters, which were h_0/e , h_0/h , and e/t_w .

The precision of the shear buckling coefficient k for the web-post buckled in elastic-plastic stage should be investigated further. The shear buckling coefficients of the web-post in a CSB with hexagonal web openings that buckled in elastic-plastic stage obtained using FEM and the design curves proposed by Redwood and Demirdjjan (1998) were shown in Fig. 7. The yield strength of steel, f_y , was 345 MPa. The edge angle of opening was 60° .

Effects of web thickness on the shear buckling coefficient of a web-post at elastic-plastic stage were shown in Fig. 7(a). Dimensions of the web-post were listed in Table 5. Three t_w were studied, which were 6.0 mm, 8.0 mm

Table 5 Dimensions of web-post to study effects of t_w on k

Group No.	e/t_w	h_0/e	h_0/h	t_w (mm)	e (mm)	h_0 (mm)	h (mm)
1				6.0	120	360,480,600,720,840,960,	480,640,800,960,1120,1280
2	20	3,4,5,6,7,8	0.74	8.0	160	480,640,800,960,1120,1280	640,853,1066,1280,1493,1706
3				10.0	200	600,800,1000,1200,1400,1600	800,1066,1333,1600,1866,2133

Table 6 Dimensions of web-post to study effects of h_0/h on k

Group No.	e/t_w	h_0/e	h_0/h	t_w (mm)	e (mm)	h_0 (mm)	h (mm)
1		3, 4, 5, 6, 7, 8	0.74		120	360,480,600,720,840,960,	480,640,800,960,1120,1280
4	20	5, 6, 7, 8	0.51	6.0	120	360,480,600,720,840,960	720,960,1200,1440,1680,1920

and 10.0 mm. For the web-posts having same e/t_w , h_0/e and h_0/h , the shear buckling coefficients k proposed by Redwood and Demirdjjan (1998) would be the same. However, as what had been demonstrated in elastic stage (Wang *et al.* 2016), FEM results showed that k changed with the changes of t_w . Hence, it was not enough to formulate the buckling coefficient by only using the three dimensionless parameters e/t_w , h_0/e and h_0/h . Furthermore, the design curves (Redwood and Demirdjjan 1998) were used to predict the elastic shear buckling strength of a web-post. It also lacked measures to distinguish whether the CSB was failed by web-post shear buckling or by Vierendeel mechanism.

Effects of h_0/h on the shear buckling coefficients of the web-post at plastic stage were shown in Fig. 7(b). Dimensions of the web-post studied were listed in Table 6. Two h_0/h were studied, which were 0.74 and 0.51. It could be seen that the slope of the k line in plastic was bigger than that at elastic stage, as shown in Fig. 7(b). Likewise, k obtained by Redwood and Demirdjjan (1998) were still much more conservative than FEM results using the sub-model.

Effects of e/t_w on k were shown in Fig. 7(c). Dimensions of the web-post studied were listed in Table 7. Two e/t_w were studied, while t_w was kept constant. At elastic stage, k decreased with the increase in e/t_w , while at plastic stage the trend was opposite, as shown in Fig. 7(c). FEM results showed that k increased with the increase in e/t_w , if the web-post had the same t_w . k obtained by Redwood and Demirdjjan (1998) were much more conservative than FEM results because effects of post-buckling strength were not included.

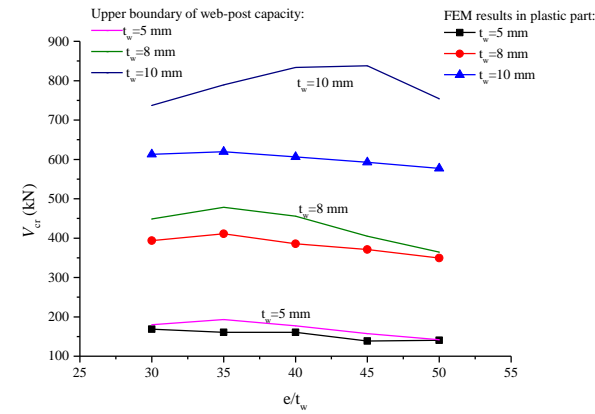
4. Parameter studies of elastic-plastic shear buckling strength of web-post

4.1 Parameters affecting elastic-plastic shear buckling strength of web-post

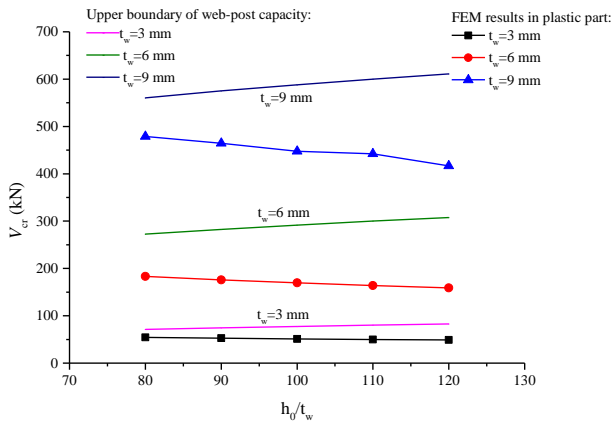
CSBs listed in Table 8-Table 12 were studied to show effects of web-post dimensions on elastic-plastic shear buckling strength of a CSB with hexagonal web openings.

Table 7 Dimensions of web-post to study effects of e/t_w on k

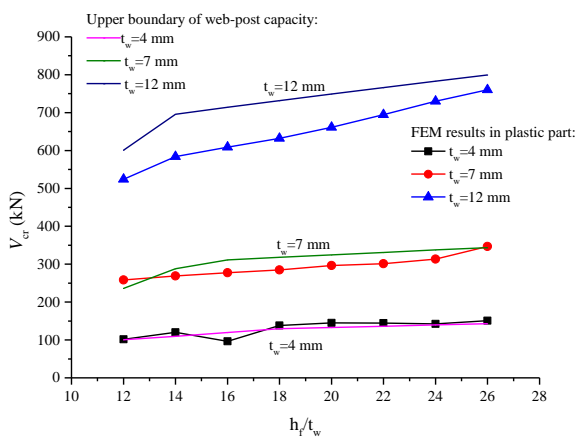
Group No.	e/t_w	h_0/e	h_0/h	t_w (mm)	e (mm)	h_0 (mm)	h (mm)
1	20	3, 4,	0.74	6.0	120	360,480,600,	480,640,800,
						720,840,960,	960,1120,1280
5	15	7, 8			90	270,360,450,	480,600,720,
						540,630,720	840,960



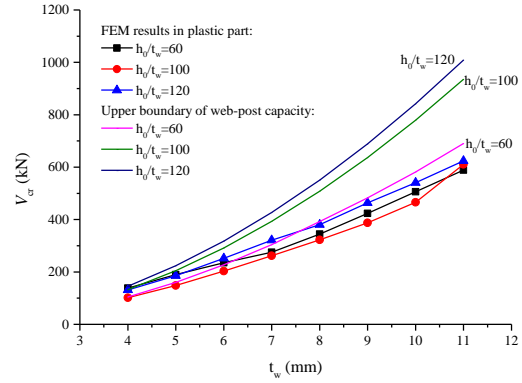
(a) Effects of e/t_w on shear buckling strength



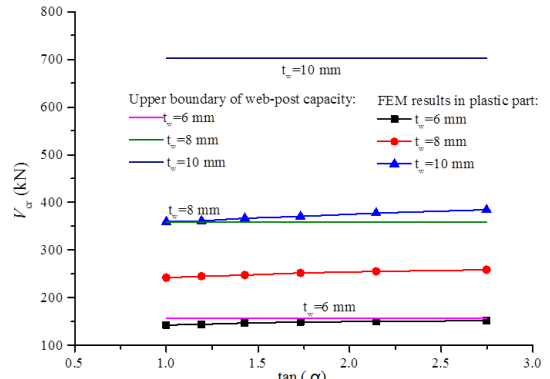
(b) Effects of h_0/t_w on shear buckling strength



(c) Effects of h_f/t_w on shear buckling strength



(d) Effects of t_w on shear buckling strength



(e) Effects of α on shear buckling strength

Fig. 8 Continued

Table 8 Parameters of sub-models for studying effects of e/t_w

Group No.	Inclination angle α	e/t_w	h_0/t_w	h_f/t_w	t_w (mm)	e (mm)	h_0 (mm)	h_f (mm)
Group I	60°	30,	100	20	5.0	150,175,	500	100
		35,				200,225,250		
Group II	60°	40,	80	25	8.0	240,280,	640	200
		45,				320,360,400		
Group III	60°	50,	90	30	10.0	300,350,	900	300
		55,				400,450,500		

inclination angle of web opening edge α .

As shown in Fig. 8(a) and 8(b), with the increase in e/t_w and h_0/t_w , the elastic-plastic shear buckling strength decreased. Unlike that at elastic stage (Wang *et al.* 2016), the elastic-plastic shear buckling strength increased with the h_f/t_w increased, as shown in Fig. 8(c). And with the increase in t_w and α , the elastic-plastic shear buckling strength increased, as shown in Fig. 8(d) and Fig. 8(e).

4.2 Effects of parameters on elastic-plastic shear buckling coefficient k

After V_{cr} was obtained through FEM simulation, the buckling coefficient k can be obtained by Eq. (4).

4.2.1 Effects of e/t_w on k

Three groups of sub-models were studied to show effects of e/t_w on k . Parameters of the studied CSBs were listed in Table 8. As shown in Fig. 9, k decreased linearly

Fig. 8 Effects of web-post dimensions on vertical shear buckling strength of the web-post

Analysis results were shown in Fig. 8. Dimensions of the web-post were represented by five parameters, which were e/t_w , h_0/t_w , h_f/t_w , the web thickness t_w (in mm), and the

Table 9 Parameters of sub-models for studying effects of h_0/t_w

Group No.	Inclination angle α	e/t_w	h_0/t_w	h_f/t_w	t_w (mm)	e (mm)	h_0 (mm)	h_f (mm)
Group IV	60°	50	80,90,	15	3.0	150	240,270, 300,330,360	45
Group V		40		20	6.0	240	480,540, 600,660,720	120
Group VI		30	25	9.0	270	720,810, 900,990,1080	225	

Table 10 Parameters of sub-models for studying effects of h_f/t_w

Group No.	Inclination angle α	e/t_w	h_0/t_w	h_f/t_w	t_w (mm)	e (mm)	h_0 (mm)	h_f (mm)
Group VII	60°	40	100	12,14,16,	4.0	160	400	48,56,64,72, 80,88,96,104
Group VIII		25	120		18,20,22,	7.0	175	840
Group IX		20	80	24,26	12.0	240	960	144,168,192,216, 240,264,288,312

with the increase in e/t_w , which meant that with the increase in e/t_w , the shear buckling strength of the web-post calculated by Eq. (4a) was overestimated. The relationship between k and e/t_w could be expressed by a linear function.

4.2.2 Effects of h_0/t_w on k

Totally 15 sub-models listed in Table 9 were studied to show effects of h_0/t_w on k . As shown in Fig. 10, k increased linearly with the increase in h_0/t_w . That is, the shear buckling strength of the web-post calculated by Eq. (4a) was underestimated with the increase in h_0/t_w . The relationship between k and h_0/t_w could be formulated by a linear function.

4.2.3 Effects of h_f/t_w on k

24 sub-models were studied to illustrate effects of h_f/t_w on k . Dimensions of sub-models studied were listed in Table 10. As shown in Fig. 11, k increased linearly with the increase in h_f/t_w . The shear buckling strength of the web-post calculated by Eq. (4a) was underestimated with the increase in h_f/t_w . The relationship between k and h_f/t_w could be formulated by a linear function.

4.2.4 Effects of t_w on k

As listed in Table 11, 24 sub-models were studied to show effects of t_w on k . As shown in Fig. 12, k decreased non-linearly with the increase in t_w , which meant the shear buckling strength of the web-post calculated by Eq. (4a) was overestimated with the increase in t_w . The relationship

Table 11 Parameters of sub-models for studying effects of t_w

Group No.	Degrees α	e/t_w	h_0/t_w	h_f/t_w	t_w (mm)	e (mm)	h_0 (mm)	h_f (mm)
Group X	60°	30	60	20	4.0,5.0,6.0, 7.0,8.0, 9.0, 10.0, 11.0	120,150,180,210,	240,300,360,420,	80,100,120,140,
Group XI						240,270,300,330	480,540,600,660	160,180,200,220
Group XII						160,200,240,280, 320,360,400,440	800,900,1000,1100	160,180,200,220
Group XII	35	120	30			140,175,210,245, 280,315,350,385	480,600,720,840, 960,1080,1200,1320	120,150,180,210, 240,270,300,330

Table 12 Parameters of sub-models for studying effects of α

Group No.	Inclination angle α	Tangent value	e/t_w	h_0/t_w	h_f/t_w	t_w (mm)	e (mm)	h_0 (mm)	h_f (mm)
Group XIII	70°, 65°, 60°, 55°, 50°, 45°	2.14,	15	80	15	6.0	90	480	90
Group XIV		1.73,	20	100	20	8.0	160	800	160
Group XV		1.43, 1.20,1.0	25	120	30	10.0	250	1200	300

between k and t_w could be formulated by a quadratic function.

4.2.5 Effects of α on k

18 sub-models were studied to show effects of α on k , as listed in Table 12. α was represented by its tangent value $\tan(\alpha)$. As shown in Fig. 13, k increased linearly with the increase in $\tan(\alpha)$. The shear buckling strength of the web-post calculated by Eq. (4a) was underestimated with the increase in $\tan(\alpha)$. The relationship between k and $\tan(\alpha)$ could be formulated by a linear function.

4.3 Practical equations for calculating shear buckling coefficient

Parameter studies showed that k decreased linearly with the increase in e/t_w as shown in Fig. 9. It increased linearly with the increase in h_0/t_w , h_f/t_w and α , as shown in Fig. 10, Fig. 11, and Fig. 13. It changed non-linearly with t_w (in mm), as shown in Fig. 12. As results of numerical regression analysis, k could be calculated by

$$k = k_1 \cdot k_2 \cdot k_3 \cdot k_4 \cdot k_5 \quad (15)$$

where

$$k_1 = 2.27 - 0.017 \frac{e}{t_w} \quad (16)$$

$$k_2 = -0.008 + 0.00041 \frac{h_0}{t_w} \quad (17)$$

$$k_3 = 1.24 + 0.021 \frac{h_f}{t_w} \quad (18)$$

$$k_4 = 64.38 - 6.131t_w + 0.314t_w^2 \quad (19)$$

$$k_5 = 2.00 + 0.021 \tan \alpha \quad (20)$$

Comparisons of k obtained from FEM and Eq. (15) were shown in Fig. 9-Fig. 13. Fig. 14 showed differences between k obtained by Eq. (15) and the sub-model FEM. Here, k_{CAL} was obtained by Eq. (15) and k_{FEM} was obtained

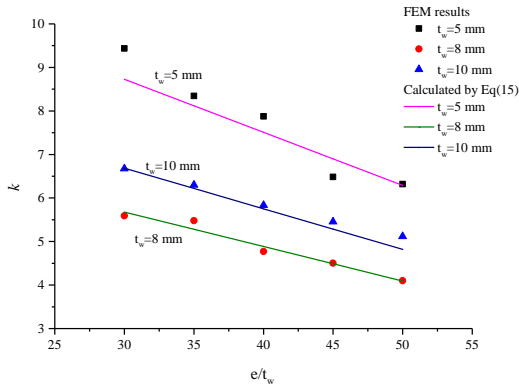


Fig. 9 Effects of e/t_w on k

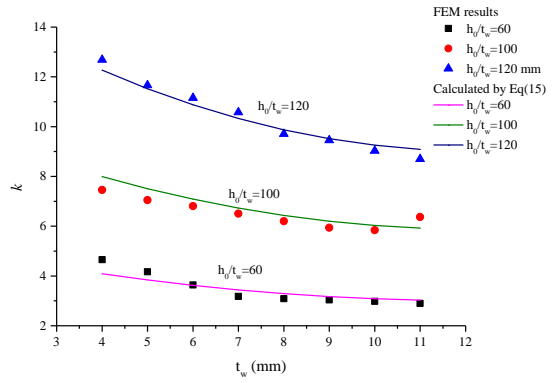


Fig. 12 Effects of t_w on k

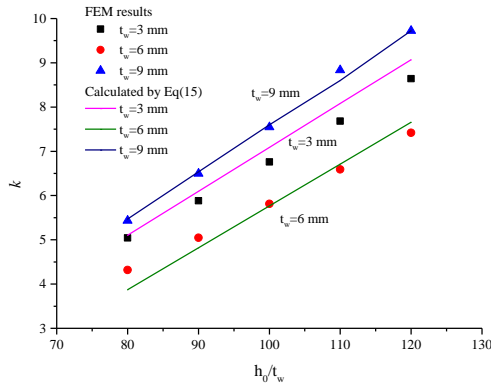


Fig. 10 Effects of h_0/t_w on k

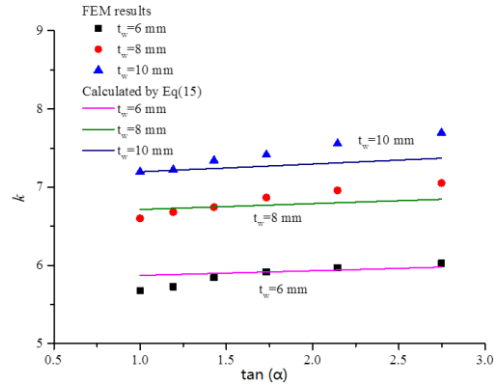


Fig. 13 Effects of α on k

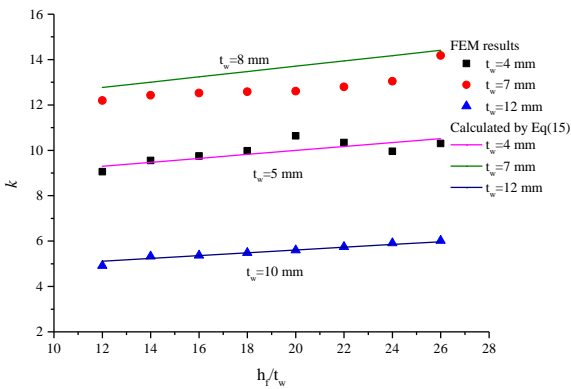


Fig. 11 Effects of h/t_w on k

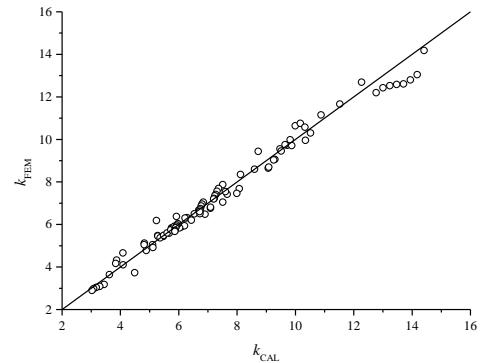


Fig. 14 Distribution of k obtained from proposed method and FEM

from the sub-model FEM analyses. k_{CAL} and k_{FEM} scattered around the $y=x$ line, which meant k_{CAL} agreed well with k_{FEM} .

5. Verification

5.1 Verification with test results

The vertical elastic-plastic shear buckling strength of the web-post in a CSB was predicted by Eq. (4b) or Eq. (3), where k was calculated by Eq. (15). Comparisons of $V_{cr,CAL}$ obtained by Eq. (4b) and the whole web-post FEM analysis were shown in Fig. 15. It could be seen that, for CSBs listed in Table 8-Table 12, $V_{cr,CAL}$ obtained by Eq. (4b) agreed well

with the whole web-post FEM analyses.

Tests results on CSBs with hexagonal openings (Redwood and Demirdjian 1998, Zaarour and Redwood 1996) were used to validate the proposed method. Calculated parameters of CSBs and shear buckling strengths of CSBs obtained from the proposed method and test were listed in Table 13. The values of $V_{cr,CAL}/P_{TEST}$ varied from 0.878 to 1.050, which showed the proposed design equations were precise enough.

5.2 Verification with design value using design equations (EC3 2005)

The EC3 (2005) proposed a design method based on the strut model to calculate the shear buckling strength of web-

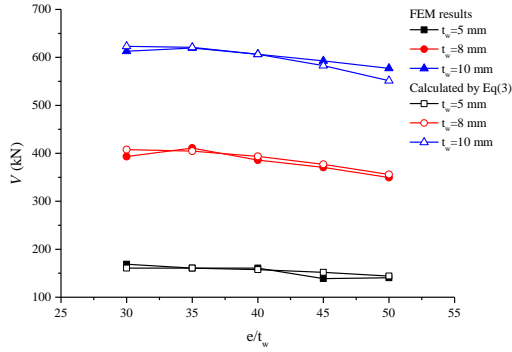
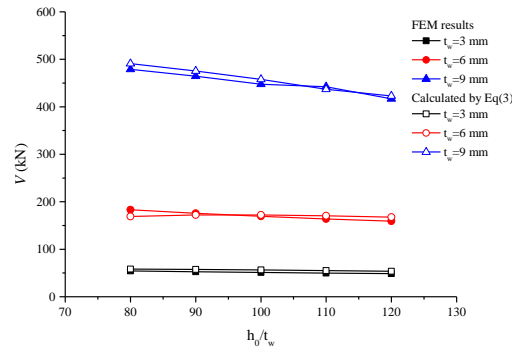
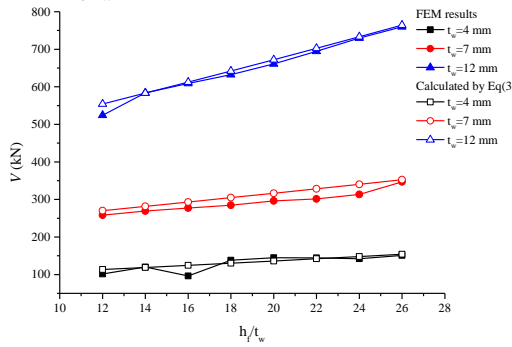

 (a) Vertical shear buckling strength of web-post with different e/t_w

 (b) Vertical shear buckling strength of web-post with different h_0/t_w

 (c) Vertical shear buckling strength of web-post with different h/t_w

 Fig. 15 Comparisons of V_{cr} obtained by proposed method and whole web-post FEM

post, where the web-post of a CSB with circular openings was treated as small strut which bear compression. The shear buckling capacity could be calculated related to the effective strut width and the effective strut length as

$$\frac{V_v}{2} = p_c \cdot b_e \cdot t_w = \chi \cdot \beta_A \cdot A \cdot p_y / \gamma_{M1} \quad (21)$$

$$\chi = \frac{1}{\phi + [\phi^2 - \bar{\lambda}^2]^{0.5}} \leq 1 \quad (22)$$

$$\phi = 0.5 \left[1 + \alpha' (\bar{\lambda} - 0.2) + \bar{\lambda}^2 \right] \quad (23)$$

$$\bar{\lambda} = [\beta_A \cdot A \cdot p_y / N_{cr}]^{0.5} \quad (24)$$

$$N_{cr} = \frac{\pi^2 EI}{l^2} \quad (25)$$

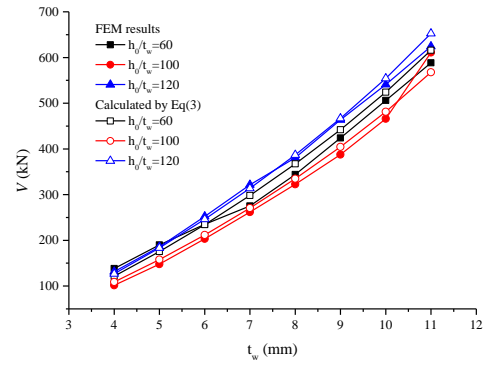
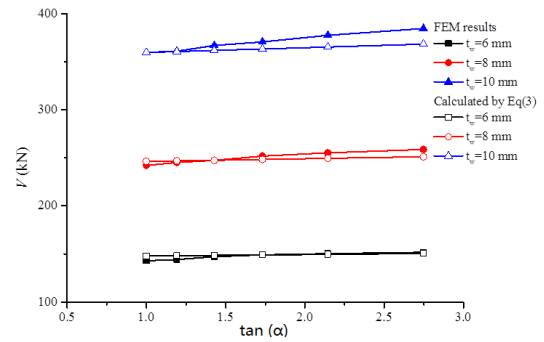

 (d) Vertical shear buckling strength of web-post with different t_w

 (e) Vertical shear buckling strength of web-post with different α

Fig. 15 Continued

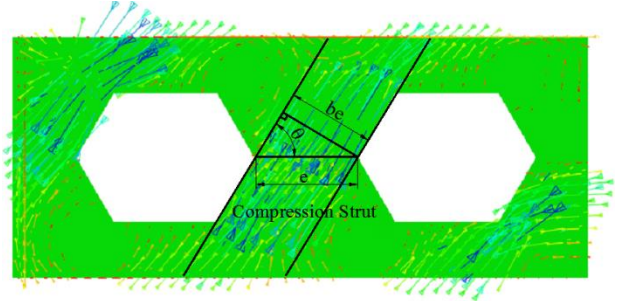


Fig. 16 Compression strut width of CSB with hexagonal openings

$$l_e = 0.5 \sqrt{e^2 + h_o^2} \quad (26)$$

$$b_e = e / 2 \quad (27)$$

where β_A was the correction factor for the lateral torsional buckling curves for rolled sections. γ_{M1} was the partial factor for resistance of members to instability assessed by member checks. p_c was the compressive strength of steel. p_y was the yield strength of steel. A was the effective area of a cross section. And, χ was the reduction factor for the relevant buckling curve.

For a CSB with hexagonal openings, the compression region distributed in whole web-post, as shown in Fig. 16. So the width of strut could be calculated as

$$b_e = e \cdot \sin \theta \quad (28)$$

Table 13 Calculated parameters of CSBs with hexagonal web openings

Specimens	e/t_w	h_0/t_w	h_f	h_f/t_w	t_w (mm)	α	$\tan\alpha$	y_i (mm)	s (mm)	V_{cr} (kN)	P_{TEST} (kN)	$V_{cr,CAL}/P_{TEST}$
10-5a	21.85	74.78	52.56	14.76	3.56	60.0	1.73	13.11	308.00	44.31	46.35	0.956
10-5b	21.85	74.78	52.56	14.76	3.56	60.0	1.73	13.11	308.00	44.31	50.45	0.878
10-6	21.85	74.78	52.56	14.76	3.56	60.0	1.73	13.11	308.00	44.31	47.4	0.935
10-7	21.85	74.78	52.56	14.76	3.56	60.0	1.73	13.11	308.00	44.31	42.2	1.050
10-1	16.25	68.68	57.97	16.19	3.58	60.0	1.73	14.86	256.04	38.22	39.55	0.966
10-3	16.04	72.17	53.50	14.82	3.61	45.0	1.00	13.26	369.82	37.92	36.92	1.027
12-1	15.65	75.23	56.39	12.02	4.69	60.0	1.73	14.62	350.02	55.74	57.33	0.972
12-3	15.45	65.48	68.19	14.76	4.62	45.0	1.00	18.46	441.44	58.16	58.22	0.999

Table 14 Calculated parameters of CSBs with hexagonal web openings

Group No.	e/t_w	h_0/t_w	h_f/t_w	t_w (mm)	α	$\tan\alpha$	V_{FEM} (kN)	V_{CAL} (kN)	V_{CAL}/V_{FEM}	V_{EC3} (kN)	V_{EC3}/V_{FEM}
Group IV		80				1.73	55.30	58.32	1.05	54.45	0.93
		90				1.73	53.56	57.51	1.07	46.69	0.87
	50	100	15	3	60°	1.73	53.09	56.32	1.06	40.29	0.76
		110				1.73	51.86	54.96	1.05	35.03	0.67
		120				1.73	50.80	53.51	1.05	30.63	0.60
Group V		80				1.73	179.27	169.04	0.95	168.78	0.94
		90				1.73	175.71	172.25	0.98	161.60	0.91
	40	100	20	6	60°	1.73	169.52	172.30	1.01	137.88	0.81
		110				1.73	163.74	170.52	1.04	118.71	0.72
		120				1.73	159.07	167.69	1.05	103.07	0.64

Table 15 Details of the specimens used as experimental validation data of the FEM model

Specimen	Original section	f_y (MPa)	h	d_0	s	l	
NB1 (Tsavdaridis and D'Mello 2011)	UB457 ×152×52	375.3	359.7	449.8	315	410	1700
NB2 (Tsavdaridis and D'Mello 2011)	UB457 ×152×52	375.3	359.7	449.8	315	378	1700
NB5 (Surtees and Liu 1995)	IPE400	300	300	558	358	480	1897
NB6 (Warren 2001)	HEB400	300	300	599	422	485	1940
NB7 (ECSC 2003)	IPE400	300	300	600	430	485	1944
NB8 (ECSC 2003)	IPE300/ HEB300	300	300	482	354	409	1644
NB9 (ECSC 2003)	HEA300/ HEB300	300	300	415	300	447	1800

Group IV and V were adopted to compare the calculated results obtained from the Eq. (4b) and from design equations in EC3 (2005), as listed in Table 14. Here, V_{CAL} was the result obtained from Eq. (4b), while V_{EC3} was the result obtained from EC3 (2005). The calculated results obtained from the Eq. (4b) matched well with the FEM results while the shear buckling strength obtained from improved EC3 (2005) design method were too conservative compared with FEM results, which revealed that the equation proposed by EC3 (2005) based on strut model has some limitation.

5.3 Verification with design value using design equations (Panedpojaman et al. 2014)

Panedpojaman et al. (2014) proposed novel design

Table 16 Comparison of the predicted shear strength to the test results

Specimen	Test (kN)	V_{cal} (kN)		V_{cal}/V_{Test}	
		Panedpojaman et al. (2014)	Proposed Eq. (4b)	Panedpojaman et al. (2014)	Proposed Eq. (4b)
NB1 (Tsavdaridis and D'Mello 2011)	144	154	139.2	1.069	0.967
NB2 (Tsavdaridis and D'Mello 2011)	128	124	121.7	0.969	0.951
NB5 (Surtees and Liu 1995)	268	215	252.5	0.802	0.942
NB6 (Warren 2001)	313	224	297.3	0.716	0.950
NB7 (ECSC 2003)	132	108	124.6	0.818	0.944
NB8 (ECSC 2003)	196	131	180.9	0.668	0.923
NB9 (ECSC 2003)	342	241	315.4	0.705	0.922
Mean value				0.821	0.943
Standard error				0.056	0.006
Standard deviation				0.148	0.016
Variance				0.022	0.000
Coefficient of variation				0.181	0.017

equations for shear strength of local web-post buckling in cellular beams. The design was based on the strut model and codes of EC3 (2005). Through incorporating the restraint effects of the tee depth and the stress variation, Panedpojaman et al. (2014) proposed a modified factor to the strut length of the strut model.

$$l_{e,PPM} = \mu l$$

$$\mu = 0.90 \frac{s}{d_0} \left(\frac{d_0}{d} \right)^2 \leq \min \left(1.15 \frac{d_0}{d}, 1.15 \right) \quad (29)$$

To assess the validity of the proposed Eq. (4b), the shear buckling strengths of web-posts in castellated steel beams listed in Table 15 were analyzed using the methods provided by Panedpojaman *et al.* (2014) and Eq. (4b). Lawson *et al.* (2006) had also provide design method for web-post shear buckling strength of castellated steel beams. It was more conservative compared with the method of Panedpojaman *et al.* (2014). So they were not listed in Table 16. Calculated results and test results on these specimens were listed in Table 16. It could be seen that the design method proposed by Panedpojaman *et al.* (2014) greatly improved the precision of EC3 (2005). However, shear buckling strength calculated by Eq. (4b) proposed here agreed much better with the test results.

6 Conclusions

Elastic-plastic buckling behaviors of the web-post in the CSB under vertical shear were investigated using finite element method based on a sub-model that the classic thin-plate shear buckling theory could be used. The sub-model treated the upper part of the web-post as a free body under horizontal shear force. Then the vertical elastic-plastic shear buckling strength of the web-post was obtained after providing the shear buckling coefficient k .

The shear buckling coefficient k was affected by the dimensionless parameters of the web-post, including e/t_w , h_0/t_w , h_f/t_w , and t_w , and opening edge angle α . k was calculated through back analysis after the vertical shear buckling strength of the web-post was obtained through the sub-model FEM. Parameters e/t_w , h_0/t_w , and h_f/t_w , t_w and α all had great influences on the shear buckling coefficient k . Through curve fitting the FEM simulation results, a simplified method was proposed to calculate k .

The calculated vertical elastic-plastic shear buckling strength of the web-post employing the proposed k agreed well with the whole castellated beam FEM result. Differences between the k calculated by proposed equations and the numerical simulations mainly lay within $\pm 5\%$. And the maximum error of k was 10%, which only occurred in one of 96 specimens. Comparisons of shear buckling strengths using the proposed coefficient k and those using EC3 design equations showed that the EC3 underestimated the shear buckling strength of a web-post greatly.

The proposed equation for calculating the elastic-plastic shear buckling strength of web-posts was derived from the CSBs with hexagonal web openings. Whether the CSBs with other web opening shapes could use the proposed equation needed to be investigated later.

Acknowledgements

The authors wish to acknowledge the support from the National Natural Science Foundation of China (51578322, 51608305), the Natural Science Foundation of Shandong Province (ZR2015EM041, 2016GGX103013) for the work reported in this paper.

References

- ABAQUS (2008), ABAQUS Standard User's Manual, Hibbit, Karlsson and Sorensen, Inc. 1, 2 and 3, Version 6.8-1, USA.
- Abidin, A.R.Z. and Izzuddin, B.A. (2013), "Meshless local buckling analysis of steel beams with irregular web openings", *Eng. Struct.*, **50**(1), 197-206.
- Abidin, A.R.Z., Izzuddin, B.A. and Lancaster, F. (2017), "A meshfree unit-cell method for effective planar analysis of cellular beams", *Comput. Struct.*, **182**(1), 368-391.
- BS5950-1 (2000), Structural Use of Steelworks in Building, British Standard Institution.
- Chung, K.F., Liu, T.C.H. and Ko, A.C.H. (2011), "Investigation on Vierendeel mechanism in steel beams with circular web openings", *J. Constr. Steel Res.*, **57**(5), 467-490.
- Durif, S., Bouchair, A. and Bacconnet, C. (2015), "Elastic rotational restraint of web-post in cellular beams with sinusoidal openings", *Steel Compos. Struct.*, **18**(2), 325-344.
- EC3 (2005), "EN 1993-1-1: Eurocode 3: Design of steel structures, Part 1.1: General rules and rules for building", UK.
- ECSC (2003), "Large web openings for service integration in composite floors", Final Report for ECSC Research Contract 7210-PR-315.
- Ellobody E. (2011), "Interaction of buckling modes in castellated steel beams", *J. Constr. Steel Res.*, **67**(5), 814-825.
- Erdal, F. and Saka, M.P. (2013), "Ultimate load carrying capacity of optimally designed steel cellular beams", *J. Constr. Steel Res.*, **80**(1), 355-368.
- Kaveh, A. and Ghafari, M.H. (2016), "Optimum design of steel floor system: effect of floor division number, deck thickness and castellated beams", *Struct. Eng. Mech.*, **59**(5), 933-950.
- Kaveh, A. and Ghafari, M.H. (2017), "Optimum design of castellated beams: effect of composite action and semi-rigid connections", *Scientia Iranica*, DOI: 10.24200/SCI.2017.4195.
- Kaveh, A. and Shokohi, F. (2015), "Optimum design of laterally-supported castellated beams using CBO algorithm", *Steel Compos. Struct.*, **18**(2), 305-324.
- Kaveh, A. and Shokohi, F. (2016a), "Optimum design of laterally-supported castellated beams using tug of war optimization algorithm", *Struct. Eng. Mech.*, **58**(3), 533-553.
- Kaveh, A. and Shokohi, F. (2016b), "A hybrid optimization algorithm for the optimal design of laterally-supported castellated beams", *Scientia Iranica*, **23**(2), 508-519.
- Kerdal, D. and Nethercot, D. (1984), "Failure modes for castellated beams", *J. Constr. Steel Res.*, **4**(4), 295-315.
- Lawson, R.M. and Hicks, S.J. (2005), "Developments in composite construction and cellular beams", *Steel Compos. Struct.*, **5**(2), 193-202.
- Lawson, R.M., Lim, J., Hicks, S.J. and Simms, W.I. (2006), "Design of composite asymmetric cellular beams and beams with large web openings", *J. Constr. Steel Res.*, **62**(6), 614-629.
- Lawson, R.M., Oshatogbe, D. and Newman, G.M. (2006), "Design of FABSEC cellular beams in non-composite and composite applications for both normal temperature and fire engineering conditions", *Cellular Beam Software: FBeam 2006 Design Guide*, Fabsec Limited Publication.
- Liu, T.C.H. and Chung, K.F. (2003), "Steel beams with large web openings of various shapes and sizes: Finite element investigation", *J. Constr. Steel Res.*, **59**(9), 1159-1176.
- Panedpojaman, P., Thepchatri, T. and Limkatanyu, S. (2014), "Novel design equations for shear strength of local web-post buckling in cellular beams", *Thin Wall. Struct.*, **76**(1), 92-104.
- Panedpojaman, P., Thepchatri, T. and Limkatanyu, S. (2015), "Novel simplified equations for Vierendeel design of beams with (elongated) circular openings", *J. Constr. Steel Res.*, **112**(1), 10-21.
- Redwood, R.G. and Demirdjian, S. (1998), "Castellated beam web

- buckling in Shear”, *J. Struct. Eng.*, ASCE, **124**(8), 1202-1207.
- Surtees, J.O. and Liu, Z. (1995), “Report of loading tests on cell-form beams”, Research Report University of Leeds.
- Tsavidaridis, K.D. and D’Mello, C. (2011), “Web buckling study of the behavior and strength of perforated steel beams with different novel web opening shapes”, *J. Constr. Steel Res.*, **67**(10), 1605-1620.
- Wang, P.J., Guo, K.R., Liu, M. and Zhang, L.L. (2016), “Shear buckling strengths of web-posts in a castellated steel beam with hexagonal web openings”, *J. Constr. Steel Res.*, **121**(1), 173-184.
- Wang, P.J., Ma, Q.J. and Wang, X.D. (2014b), “Investigation on Vierendeel mechanism failure of castellated steel beams with fillet corner web openings”, *Eng. Struct.*, **74**(1), 44-51.
- Wang, P.J., Wang, X.D. and Ma, N. (2014a), “Vertical shear buckling capacity of web-posts in castellated steel beams with fillet corner hexagonal web openings”, *Eng. Struct.*, **75**(1), 315-326.
- Warren, J. (2001), “Ultimate load and deflection behaviour of cellular beams”, MSc. Thesis, Durban: School of Civil Engineering, University of Natal.
- Yang, Y., Yu, Y.L., Guo, Y.X., Roeder, C.W., Xue, Y.C. and Shao, Y.J. (2016), “Experimental study on shear performance of partially precast Castellated Steel Reinforced Concrete (CPSRC) beams”, *Steel Compos. Struct.*, **21**(2), 289-302.
- Zaarour, W. and Redwood, R.G. (1996), “Web buckling in thin webbed castellated beams”, *J. Struct. Div.*, ASCE, **122**(8), 860-866.